# Use of specific contrast-enhanced CT regions of interest to differentiate renal oncocytomas from small clear cell and chromophobe renal cell carcinomas

Jian-Yi Qu* [ID]
Hong Jiang* [ID]
Xiao-Fei Wang [ID]
Xin-Hong Song [ID]
Cui-Juan Hao [ID]

**PURPOSE**
We aimed to examine the usefulness of utilizing a specific contrast-enhanced computed tomography (CT) region of interest (ROI) to differentiate renal oncocytoma (RO) from small clear cell renal cell carcinoma (ccRCC) and chromophobe renal cell carcinoma (chRCC).

**METHODS**
A retrospective analysis of pre-contrast phase (PCP), corticomedullary phase (CMP), and nephrographic phase (NP) contrast-enhanced CT images of the histopathologically confirmed initial cohort (27 ROs, 74 ccRCCs, and 36 chRCCs) was conducted. Small, medium, large, and whole ROIs (S-ROI, M-ROI, L-ROI, and W-ROI, respectively) were utilized for CT attenuation value of tumor (AVT), lesion-to-cortex attenuation (L/C), and heterogeneous degree of tumor (HDT) calculations. Differences in these parameters were then compared between RO and ccRCC/chRCC, with receiver operating characteristic (ROC) curves being utilized to gauge the diagnostic utility of the statistically significant parameters. Logistic regression analyses were employed to identify key factors capable of differentiating RO and ccRCC/chRCC, with predictive models further being established. A validation cohort (6 ROs, 30 ccRCCs, and 12 chRCCs) was then employed to validate the performance of the predictive models.

**RESULTS**
Of the parameters evaluated using different ROIs, L/C-CMP (S-ROI) ($0.88 \pm 0.15$ vs. $1.13 \pm 0.25$, $P < .001$) and HDT-CMP (W-ROI) (23.02 (12.00-51.21) vs. 37.81 (16.09-89.45), $P < .001$) were best suited to differentiating RO and ccRCC, yielding respective area under the curve (AUC) values of 0.803 and 0.834. AVT-NP (S-ROI) ($122.85 \pm 18.87$ vs. $86.50 \pm 18.65$, $P < .001$) and AVT-NP (M-ROI) (119 (86-167) vs. 81.5 (53-142), $P < .001$) were better able to differentiate RO and chRCC, yielding respective AUC values of 0.918 and 0.906. Logistic regression analyses revealed that L/C-CMP (S-ROI) and HDT-PCP, as well as AVT-NP (S-ROI) and HDT-CMP, were the primary factors capable of differentiating RO from ccRCC and chRCC, respectively. The predictive model developed to differentiate between RO and ccRCC exhibited a sensitivity of 66.67% and 55.14% in the initial and validation cohorts, respectively, with corresponding specificity of 94.59% and 93.55%, accuracy of 87.13% and 86.84%, and AUC of 0.908 and 0.876. The predictive model developed to differentiate between RO and chRCC exhibited a sensitivity of 85.19% and 100.00% in the initial and validation cohorts, respectively, with corresponding specificity of 94.59% and 92.86%, accuracy of 87.30% and 95.24%, and AUC of 0.944 and 0.959.

**CONCLUSION**
These data demonstrate that a combination of quantitative parameters measured with particular ROIs can enable the efficient and reliable differentiation of RO from ccRCC and chRCC for use in routine patient differential diagnosis.

From the Department of Radiology (J.-Y.Q., H.J., X.-H.S., C.-J.H. ✉ CJHao2019@163.com), Yantai Yuhuangding Hospital, Qingdao University School of Medicine, Yantai, China; Department of Urology (X.-F.W.), Yantaishan Hospital, Binzhou Medical University, Yantai, China.

*Jian-yi Qu and Hong jiang contributed equally to this work.

An estimated 20%-30% of solid masses < 4 cm in size are benign, with renal oncocytomas (ROs) accounting for over half of these cases while the remaining 70%-80% are renal cell carcinomas (RCCs), among which clear cell RCCs (ccRCCs) are the most prevalent, followed by papillary RCCs (pRCCs) and chromophobe RCCs (chRCCs).[1,2] Given that ROs exhibit a benign disease course and affected patients have an excellent prognosis, accurately differentiating between RO and RCC is critical to guide appropriate patient treatment.[3]

Computed tomography (CT) is the most common approach used for the diagnosis and evaluation of renal masses. Several reports have described the differentiation between ROs and RCCs based upon both qualitative and quantitative CT findings, with the enhancement degree and heterogeneity being 2 key indicators.[4-8] Owing to a lack of reference standard uniformity, however, these studies utilized different approaches to define the regions of interest (ROIs) to obtain CT parameter values, potentially contributing to inconsistencies or opposing findings among studies. Also, tumor heterogeneity is also considered to be a largely subjective determination of limited clinical utility.[7-8] Rosenkrantz et al.[9] found the use of a small ROI (S-ROI) to be more accurate than a large ROI (L-ROI) when differentiating between RCCs and cysts, with this approach being most effective when comparing pRCCs and cysts. Wang et al.[10] also reported that S-ROI-based enhancement degree and whole ROI (W-ROI)-based enhancement heterogeneity were superior to medium ROI (M-ROI) when differentiating between small ccRCC and fat-poor angiomyolipoma (AML).

To date, no studies have explored the use of different ROIs to differentiate between ROs and RCCs on contrast-enhanced CT images. Given that pRCCs are typically hypovascular, efforts to distinguish between ROs and RCCs are generally focused on the chRCCs and ccRCCs.[11-12] This study was thus developed to explore the effect of ROI size in differentiating ROs from ccRCCs and chRCCs in an effort to define the most effective quantitative parameters for routine differential diagnosis.

## Methods

### Patients

The institutional review board approved the present study (2021/217), with the requirement for informed consent having been waived due to the retrospective nature of these analyses. Two cohorts (an initial cohort and a validation cohort) were included in this study.

**Initial cohort:** A total of 53 patients with RO and 131 patients with chRCC were retrospectively selected from the institutional pathology database between June 2013 and January 2021. Of these 184 patients, 63 were ultimately included in this study in light of the following inclusion criteria: (i) patients who had undergone preoperative pre-contrast phase (PCP), corticomedullary phase (CMP), and nephrographic phase (NP) CT imaging; (ii) patients with tumors exhibiting the maximum axial diameter ≤ 4 cm; (iii) patients with tumors

exhibiting solid portion > 25%; and (iv) patients with tumors being confirmed by histopathology after partial or radical nephrectomy. In addition, 73 consecutive ccRCC patients evaluated over a 12-month period who met these same inclusion criteria were included as controls, yielding a final cohort consisting of 136 patients bearing 137 renal tumors, with 1 patient exhibiting 2 ccRCCs. These tumors were separated into RO (n = 27), chRCC (n = 36), and ccRCC (n = 74) groups (Figure 1).

**Validation cohort:** The validation dataset was composed of 7 patients with RO and 14 patients with chRCC between February 2021 and March 2022 as well as between January 2012 and May 2013, and 31 consecutive ccRCC patients evaluated over a 5-month period. All cases met the same inclusion criteria used for the initial dataset. The final validation dataset consisted of 52 patients bearing 52 tumors (Figure 1).

### CT examination

Philips Brilliance 64- or 256-detector row helical scanners (Philips Healthcare) were used to conduct all CT imaging. Patients were directed to hold their breath during imaging, which was conducted using consistent parameters for all patients (tube voltage: 120 kV; tube current: 150-250 mA; scanning thickness: 5 mm; reconstruction thickness: 5 mm). High-pressure automated injectors were used to administer 80-100 mL of Iohexol (General Electric Pharmaceuticals Shanghai Co., Ltd.) into an antecubital vein

**Main points**

- Quantitative computed tomography (CT) parameters measured using different regions of interest (ROIs) exhibit varying levels of diagnostic efficacy when differentiating renal oncocytoma (ROs) from small clear cell renal cell carcinomas (ccRCCs) and chromophobe renal cell carcinomas (chRCCs).

- Lesion-to-cortex attenuation- corticomedullary phase (CMP) (small ROI (S-ROI)) and attenuation value of the tumor-nephrographic phase (S-ROI) were identified as the most reliable enhancement degree-related quantitative parameters when distinguishing ROs from ccRCCs and chRCCs, respectively.

- Heterogeneous degree of tumor (HDT), which was defined based upon the standard deviation for CT values, can serve as a quantitative measure of heterogeneity when differentiating ROs from ccRCCs and chRCCs, with HDT-CMP exhibiting the highest degree of differential diagnostic efficacy.

- Predictive models combining the above S-ROI-based enhancement degree parameters and whole ROI-based HDT values exhibit excellent diagnostic efficacy when differentiating ROs from ccRCCs and chRCCs.
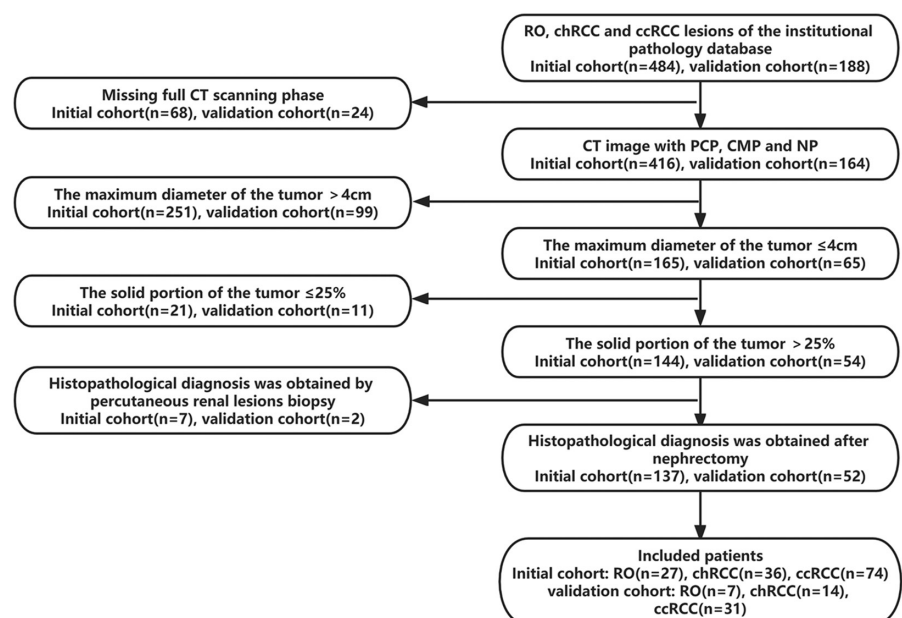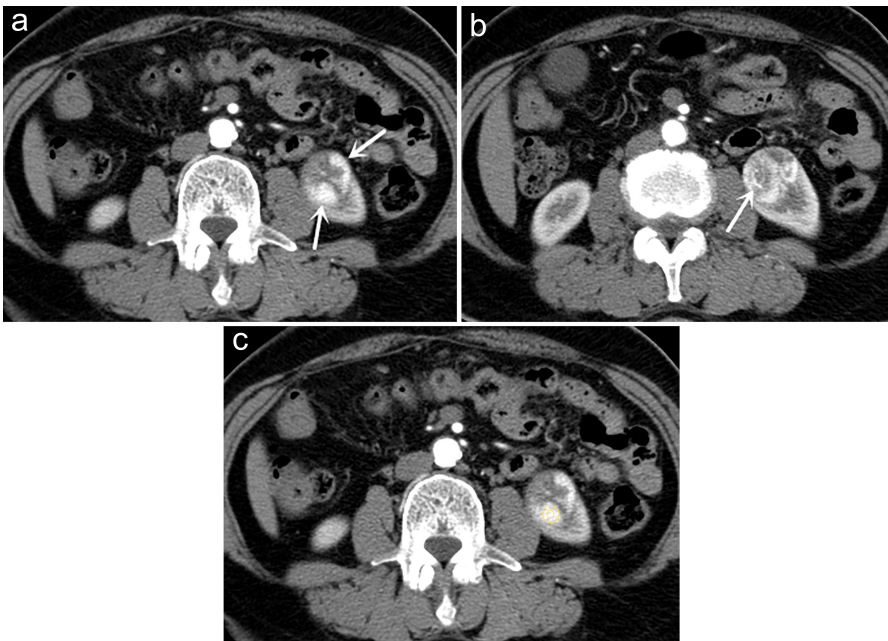


**Figure 1.** Flowchart of patient enrolment.

**Figure 2. a-c.** The placement method of S-ROI and M-ROI. **(a)** Schematic diagram of the rich blood supply area of tumor. The small pieces enhanced region was observed at the edge of tumor's parenchyma *(arrows)*. **(b)** Schematic diagram of the tumor vessel. The linear structure was observed in the tumor's parenchyma *(arrow)*. **(c)** Schematic diagram of the placement of S-ROI and M-ROI. M-ROI, medium region-of-interest; S-ROI, small region-of-interest.

at 5 mL/s, with enhanced CT scanning being conducted in CMP (25-30 second delay) and NP (60-90 second delay).

### Image analyses

**Initial cohort:** ROI placement on axial images with 5 mm slice thickness from the initial dataset was conducted through consensus between 2 blinded radiologists with 6 and 11 years of experience according to the following procedure.

First, an S-ROI (area: 10-20 mm$^2$) and an M-ROI (area: 50-100 mm$^2$) were placed in the tumor regions exhibiting the greatest degree of enhancement in CMP images (Figure 2). These 2 ROIs were placed with the following considerations: (i) S-ROI and M-ROI placement in PCP and NP images should be based on the positioning and sizing used for CMP images; (ii) regions of intratumoral vasculature, cystic degeneration, central scarring, and calcification should be avoided, with care being taken to differentiate between blood vessels and tumor-rich blood supply lesions based on previously defined morphological characteristics[10] (Figure 2); and (iii) each parameter should be measured 2 times, with the average value being recorded as the attenuation value of the tumor (AVT). An additional ROI should then be placed within the adjacent renal cortical region to measure the attenuation value of the cortex (AVC), allowing for the lesion-to-cortex attenuation (L/C) ratio to be measured as follows: (AVT/AVC) × 100%.

Second, an L-ROI was placed such that it was covering the maximum amount of enhanced tumor parenchyma possible in CMP images (Figure 3). L-ROI placement was performed under the following considerations: (i) L-ROI placement for PCP and NP images should be based on the ROI used in corresponding CMP images; (ii) areas of intratumoral calcification, cystic degeneration, and central scarring should be avoided; and (iii) all parameters should be measured 2 times, with the average values being recorded. The AVT and L/C were then calculated as mentioned earlier.

Third, W-ROI placement was performed along the largest axial NP image of the tumor in order to measure the heterogeneous degree of tumor (HDT), which was determined based upon the standard deviation (SD) of CT values (Figure 4). Since the tumor boundary was most clearly shown in NP, the HDT was measured in this phase first. W-ROI placement was performed with the following considerations: (i) W-ROI placement in PCP and CMP images should be performed with reference to NP images; (ii) W-ROIs should cover the entirety of a given tumor to the greatest extent possible, including all intratumoral components, with an edge 2-3 mm from the tumor edge; and (iii) each parameter should be measured 2 times, with the average values being recorded. The AVT and L/C were then additionally measured as mentioned earlier.

Two other radiologists with 7 and 15 years of experience placed another set of ROIs following the above methods for the inter-observer agreement calculations.
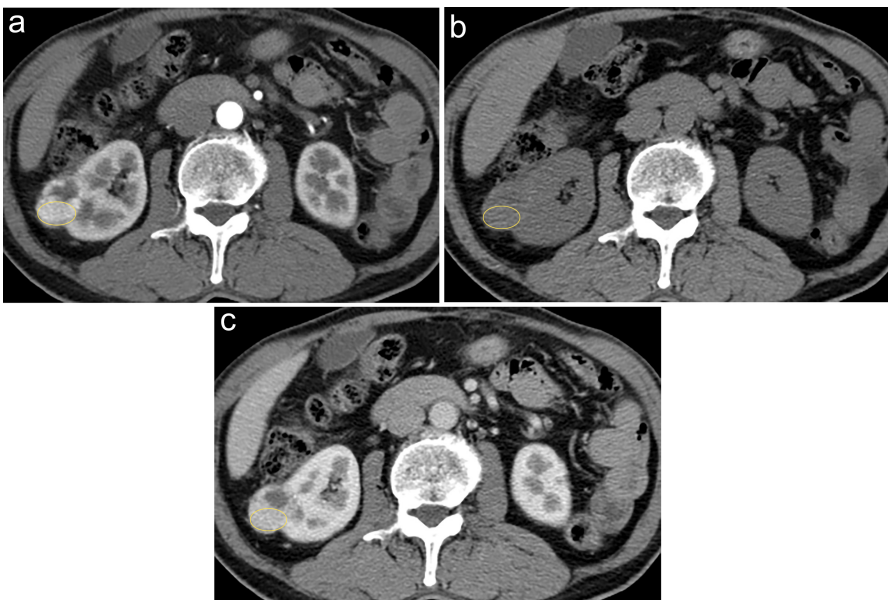


**Figure 3. a-c.** The placement method of L-ROI. **(a)** CMP, **(b)** PCP, and **(c)** NP images. ROI was first placed in the CMP image to cover the enhanced tumor parenchyma as much as possible. ROIs in PCP and NP were placed referring to the location and size of ROI in CMP. CMP, corticomedullary phase; L-ROI, large region-of-interest; PCP, pre-contrast phase; NP, nephrographic phase; ROI, region-of-interest.
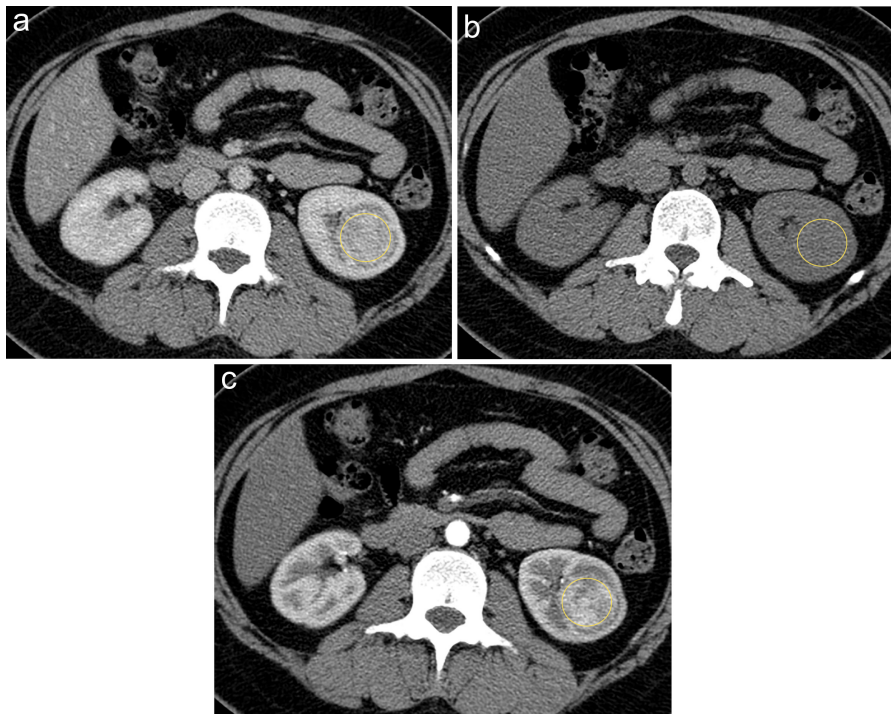
**Figure 4. a-c.** The placement method of W-ROI. **(a)** NP, **(b)** PCP, and **(c)** CMP images. ROI was first placed in the NP image to cover the whole range of tumor as much as possible, with its edge 2-3 mm away from the tumor's edge. ROIs in PCP and CMP were placed referring to the location and size of ROI in CMP. W-ROI: whole region-of-interest.

**Validation cohort:** To validate the performance of the developed predictive models, an independent radiologist with 4 years of experience analyzed the validation dataset in the same manner as the initial dataset was analyzed. The predictive models established based on the initial dataset were tested on this validation dataset. Sensitivity, specificity, accuracy, area under the curve (AUC), and 95% confidence interval (CI) values were then calculated for this validation cohort.

### Statistical analysis

Statistical Package for the Social Sciences 25.0 (IBM Inc.) was used for all statistical analyses. The Kolmogorov-Smirnov test was used to assess data normality, with normally and non-normally distributed quantitative variables being reported as mean ± SD and median (min-max), respectively, while categorical variables are given as n (%). The inter-observer agreement of quantitative data was evaluated via intraclass correlation coefficient (ICC). An ICC > 0.75 was considered to indicate a good agreement. Quantitative data were compared via independent sample t tests and Mann-Whitney U tests when normally and non-normally distributed, respectively. A $P < .05$ was the significance threshold. Receiver operating characteristic (ROC) curves were constructed for variables exhibiting significance in initial analyses, with AUC, specificity, sensitivity, and optimal cut-off values being calculated. Those parameters with $P < .01$ were then incorporated into logistic regression analyses to screen main factors for differentiating RO from ccRCC and chRCC and to establish predictive models. Sensitivity, specificity, and accuracy values were calculated for these models, with AUC (95% CI) being used to evaluate predictive performance.
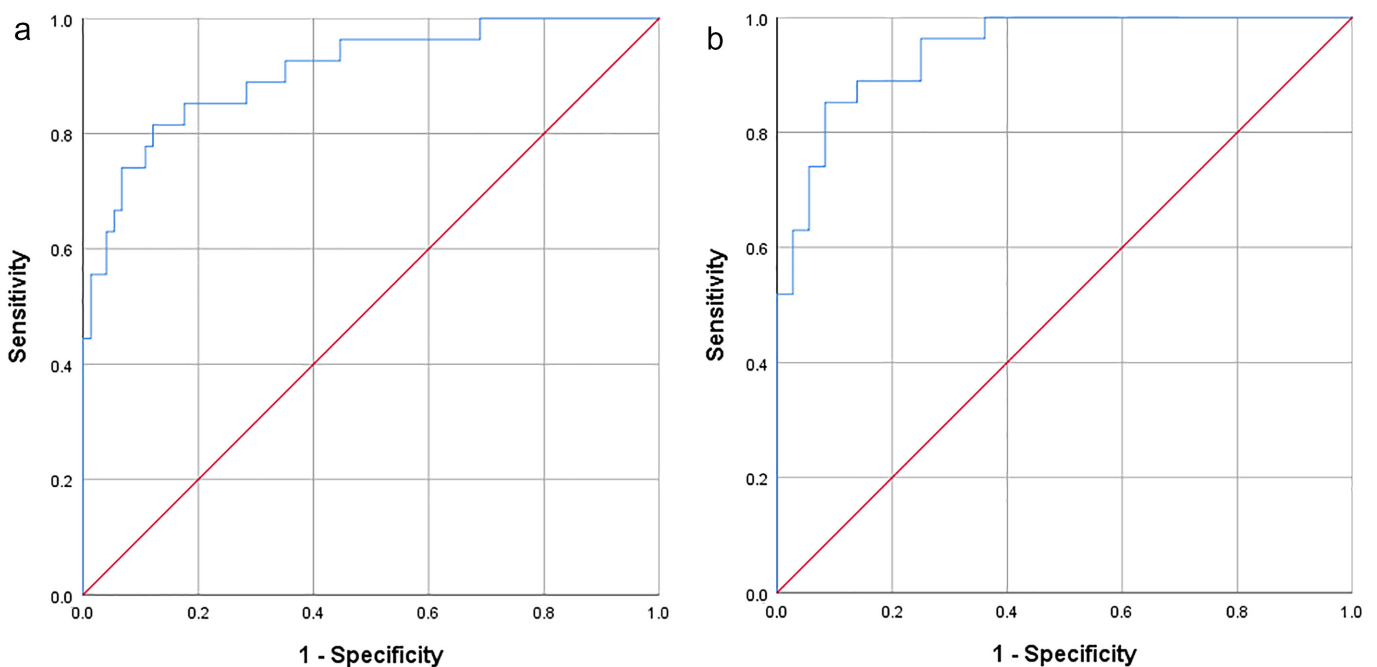


**Figure 5. a, b.** ROC curves of the prediction models. **(a)** ROC curve for differentiation of RO from ccRCC. **(b)** ROC curve for differentiation of RO from chRCC. ccRCC, clear cell renal cell carcinoma; chRCC, chromophobe renal cell carcinoma; RO: renal oncocytoma; ROC, receiver operating characteristic.

## Results

The initial cohort enrolled 60 females and 76 males (44.12% and 55.88%, respectively), with a median age of 59.5 (range: 32-85) years. The mean sizes of ROs, ccRCCs, and chRCCs were 2.69 ± 0.81 cm, 3.00 ± 0.72 cm, and 3.13 ± 0.70 cm, respectively. The ICC of quantitative data obtained by 2 teams of radiologists ranged from 0.780 to 0.988. Specifically, the ICC values for AVT-PCP, AVT-CMP, and AVT-NP measured via S-ROI were 0.780, 0.913, and 0.899, respectively.

AVT-CMP and L/C-CMP measured via S-ROI (P=.002 and P < .001, respectively), M-ROI (P=.006 and P < .001, respectively), and L-ROI (P=.041 and P=.001, respectively) differed significantly between RO and ccRCC. AVT-PCP, HDT-PCP, HDT-CMP, and HDT-NP measured via W-ROI differed significantly between RO and ccRCC (P=.025, P < .001, P < .001, and P=.001, respectively) (Table 1). Of these parameters, the highest AUC values were evident for L/C-CMP (S-ROI) and HDT-CMP (0.803 and 0.834, respectively) (Table 2).

AVT-CMP, AVT-NP, L/C-CMP, and L/C-NP measured via S-ROI, M-ROI, and L-ROI all differed significantly between RO and chRCC (all P < .001). AVT-PCP, AVT-NP, L/C-PCP, L/C-NP, HDT-PCP, HDT-CMP, and HDT-NP measured via W-ROI differed significantly between RO and chRCC (P=.005, P < .001, P=.004, P < .001, P=.025, P < .001, and P=.004, respectively) (Table 1). Of these parameters, the highest AUC values were evident for AVT-NP (S-ROI) and AVT-NP (M-ROI) (0.918 and 0.906, respectively) (Table 3).

In logistic regression analyses, L/C-CMP (S-ROI) and HDT-PCP were identified as the primary predictive factors capable of differentiating between RO and ccRCC lesions, with respective sensitivity, specificity, accuracy, and AUC (95% CI) values for the resultant predictive model of 66.67%, 94.59%, 87.13%, and 0.908 (0.840-0.976). In addition, AVT-NP (S-ROI) and HDT-CMP were identified as the primary predictive factors capable of differentiating between RO and chRCC, with respective sensitivity, specificity, accuracy, and AUC (95% CI) values for the corresponding predictive model of 85.19%, 94.59% 87.30%, and 0.944 (0.894-0.995) (Table 4 and Figure 5).

The validation cohort enrolled 24 females and 28 males (46.15% and 53.85%, respectively); the mean age ± SD was 55.40 ± 11.45 years. The mean size ± SD of ROs, ccRCCs, and chRCCs was 2.74 ± 0.76 cm, 2.69 ± 0.73 cm, and 2.96 ± 0.75 cm, respectively. Sensitivity, specificity, accuracy, and AUC (95% CI) values for the validation cohort when analyzing the predictive model used to differentiate between RO and ccRCC were 57.14%, 93.55%, 86.84%, and 0.876 (0.750-1.000), respectively, while for the model used to differentiate between RO and chRCC, these values were 100.00%, 92.86%, 95.24%, and 0.959 (0.874-1.000), respectively.

## Discussion

The results of this study indicate that quantitative parameters derived from different ROIs in contrast-enhanced CT images offer varying levels of diagnostic utility when distinguishing ROs from ccRCCs and chRCCs. Notably, the logistic regression model developed herein based upon these specific ROI-based quantitative parameters can differentiate ROs from ccRCCs and chRCCs with excellent performance.

Many quantitative CT-derived parameters have previously been shown to

**Table 1.** The comparative analysis of quantitative parameters between RO and RCC

| Parameter | RO (n = 27) | ccRCC (n = 74) | chRCC (n = 36) | RO vs ccRCC | RO vs chRCC |
|---|---|---|---|---|---|
| | | | | *P* | |
| AVT-PCP (S-ROI) | 40 (24-47) | 36 (20-54) | 38 (28-50) | .157 | .566 |
| AVT-CMP (S-ROI) | 149.59 ± 30.99 | 184.93 ± 51.10 | 110.03 ± 30.26 | .002 | <.001 |
| AVT-NP (S-ROI) | 122.85 ± 18.87 | 115.09 ± 26.94 | 86.50 ± 18.65 | .172 | <.001 |
| L/C-PCP (S-ROI) | 1.13 ± 0.21 | 1.15 ± 0.26 | 1.12 ± 0.16 | .670 | .885 |
| L/C-CMP (S-ROI) | 0.88 ± 0.15 | 1.13 ± 0.25 | 0.67 ± 0.18 | <.001 | <.001 |
| L/C-NP (S-ROI) | 0.74 (0.49-0.97) | 0.72 (0.30-1.18) | 0.50 (0.30-0.86) | .960 | <.001 |
| AVT-PCP (M-ROI) | 35.96 ± 5.45 | 33.96 ± 5.45 | 36.94 ± 5.12 | .161 | .466 |
| AVT-CMP (M-ROI) | 137.00 ± 31.46 | 165.07 ± 48.38 | 102.33 ± 30.02 | .006 | <.001 |
| AVT-NP (M-ROI) | 119 (88-167) | 112 (50-180) | 81.5 (53-142) | .174 | <.001 |
| L/C-PCP (M-ROI) | 1.00 (0.67-1.48) | 1.00 (0.59-2.40) | 1.08 (0.76-1.55) | .645 | .342 |
| L/C-CMP (M-ROI) | 0.80 ± 0.15 | 1.01 ± 0.24 | 0.62 ± 0.17 | <.001 | <.001 |
| L/C-NP (M-ROI) | 0.72 (0.52-0.95) | 0.72 (0.28-1.09) | 0.51 (0.35-0.92) | .927 | <.001 |
| AVT-PCP (L-ROI) | 36 (20-43) | 31.5 (15-51) | 37 (26-57) | .052 | .178 |
| AVT-CMP (L-ROI) | 128 (60-229) | 141.5 (35-302) | 84 (52-177) | .041 | <.001 |
| AVT-NP (L-ROI) | 122.33 ± 20.42 | 114.18 ± 28.25 | 85.89 ± 19.87 | .173 | <.001 |
| L/C-PCP (L-ROI) | 1.03 ± 0.18 | 1.00 ± 0.28 | 1.12 ± 0.18 | .643 | .051 |
| L/C-CMP (L-ROI) | 0.73 ± 0.15 | 0.89 ± 0.24 | 0.55 ± 0.16 | .001 | <.001 |
| L/C-NP (L-ROI) | 0.73 (0.51-0.93) | 0.70 (0.23-1.95) | 0.49 (0.38-0.94) | .539 | <.001 |
| AVT-PCP (W-ROI) | 32 (21-43) | 29 (18-45) | 36.5 (25-57) | .025 | .005 |
| AVT-CMP (W-ROI) | 92 (51-218) | 103 (40-244) | 80 (43-176) | .326 | .053 |
| AVT-NP (W-ROI) | 110.11 ± 19.53 | 98.95 ± 27.80 | 85.28 ± 20.75 | .058 | <.001 |
| L/C-PCP (W-ROI) | 0.96 ± 0.19 | 0.93 ± 0.24 | 1.10 ± 0.18 | .505 | .004 |
| L/C-CMP (W-ROI) | 0.52 (0.33-1.03) | 0.63 (0.35-1.22) | 0.51 (0.27-0.94) | .093 | .106 |
| L/C-NP (W-ROI) | 0.65 (0.41-0.83) | 0.63 (0.22-1.02) | 0.50 (0.34-0.94) | .350 | <.001 |
| HDT-PCP | 11.26 ± 2.89 | 14.02 ± 3.08 | 13.28 ± 3.83 | <.001 | .025 |
| HDT-CMP | 23.02 (12.00-51.21) | 37.81 (16.09-89.45) | 16.83 (9.05-30.12) | <.001 | <.001 |
| HDT-NP | 20.93 ± 8.17 | 25.92 ± 6.15 | 16.29 ± 3.68 | .001 | .004 |

S-ROI, small region-of-interest; M-ROI, medium region-of-interest; L-ROI, large region-of-interest; W-ROI, whole region-of-interest; RO, renal oncocytoma; RCC, renal cell carcinoma; ccRCC, clear cell renal cell carcinoma; chRCC, chromophobe renal cell carcinoma; AVT, attenuation value of tumor; L/C, the ratio of lesiontocortex attenuation; PCP, pre-contrast phase; CMP, corticomedullary phase; NP, nephrographic phase; HDT, heterogeneous degree of tumor.

**Table 2.** Results of ROC curves analysis for differentiation of RO and ccRCC

| Parameters | Cutoff value | Sensitivity | Specificity | AUC | SE | 95% CI |
|---|---|---|---|---|---|---|
| AVT-CMP (S-ROI) | 194 | 0.963 | 0.432 | 0.719 | 0.053 | 0.615-0.822 |
| L/C-CMP (S-ROI) | 0.99 | 0.815 | 0.784 | 0.803 | 0.044 | 0.717-0.890 |
| AVT-CMP (M-ROI) | 182.5 | 0.963 | 0.365 | 0.689 | 0.056 | 0.579-0.799 |
| L/C-CMP (M-ROI) | 0.93 | 0.852 | 0.662 | 0.773 | 0.047 | 0.681-0.866 |
| AVT-CMP (L-ROI) | 137.5 | 0.741 | 0.541 | 0.646 | 0.060 | 0.529-0.763 |
| L/C-CMP (L-ROI) | 0.77 | 0.630 | 0.770 | 0.721 | 0.053 | 0.617-0.824 |
| AVT-PCP (W-ROI) | 31.5 | 0.593 | 0.676 | 0.646 | 0.060 | 0.528-0.764 |
| HDT-PCP | 9.88 | 0.407 | 0.932 | 0.738 | 0.056 | 0.629-0.848 |
| HDT-CMP | 30.19 | 0.778 | 0.811 | 0.834 | 0.048 | 0.740-0.928 |
| HDT-NP | 20.34 | 0.593 | 0.824 | 0.716 | 0.067 | 0.585-0.847 |

S-ROI, small region-of-interest; M-ROI, medium region-of-interest; L-ROI, large region-of-interest; W-ROI, whole region-of-interest; RO, renal oncocytoma; ccRCC, clear cell renal cell carcinoma; AVT, attenuation value of tumor; L/C, the ratio of lesiontocortex attenuation; PCP, pre-contrast phase; CMP, corticomedullary phase; NP, nephrographic phase; HDT, heterogeneous degree of tumor; ROC, receiver operating characteristic; AUC, area under curve; SE, Standard error; CI, confidence interval.

offer utility for differentiating between ROs and RCCs.[11] However, ROI placement approaches have varied substantially among prior studies, resulting in inconsistent findings from different studies, particularly when comparing ROs and ccRCCs. For example, Ren et al.[5] and Young et al.,[13] respectively, placed ROIs of 8-15 mm$^2$ and 50-100 mm$^2$ in the tumor area exhibiting the greatest degree of enhancement, while Bird et al.[14] placed an ROI of 100 mm$^2$ in the area of the homogeneous tumor enhancement, and Gentili et al.[4] used an ROI encompassing the maximum amount of tumor

**Tables 3.** Results of ROC curves analysis for differentiation of RO and chRCC

| Parameters | Cutoff value | Sensitivity | Specificity | AUC | SE | 95% CI |
|---|---|---|---|---|---|---|
| AVT-CMP (S-ROI) | 119.5 | 0.852 | 0.755 | 0.836 | 0.050 | 0.738-0.935 |
| AVT-NP (S-ROI) | 104.5 | 0.852 | 0.861 | 0.918 | 0.034 | 0.852-0.984 |
| L/C-CMP (S-ROI) | 0.74 | 0.815 | 0.722 | 0.813 | 0.054 | 0.707-0.918 |
| L/C-NP (S-ROI) | 0.53 | 0.963 | 0.611 | 0.848 | 0.048 | 0.754-0.942 |
| AVT-CMP (M-ROI) | 108.5 | 0.852 | 0.694 | 0.802 | 0.057 | 0.691-0.913 |
| AVT-NP (M-ROI) | 105.5 | 0.889 | 0.889 | 0.906 | 0.039 | 0.830-0.982 |
| L/C-CMP (M-ROI) | 0.73 | 0.667 | 0.806 | 0.787 | 0.057 | 0.675-0.899 |
| L/C-NP (M-ROI) | 0.54 | 0.963 | 0.639 | 0.863 | 0.046 | 0.772-0.954 |
| AVT-CMP (L-ROI) | 107.5 | 0.778 | 0.778 | 0.797 | 0.058 | 0.683-0.911 |
| AVT-NP (L-ROI) | 104.5 | 0.852 | 0.861 | 0.892 | 0.041 | 0.813-0.972 |
| L/C-CMP (L-ROI) | 0.59 | 0.889 | 0.694 | 0.812 | 0.056 | 0.702-0.921 |
| L/C-NP (L-ROI) | 0.65 | 0.741 | 0.889 | 0.872 | 0.045 | 0.784-0.960 |
| AVT-PCP (W-ROI) | 33.0 | 0.519 | 0.833 | 0.685 | 0.070 | 0.548-0.822 |
| AVT-NP (W-ROI) | 90.5 | 0.815 | 0.694 | 0.812 | 0.055 | 0.703-0.920 |
| L/C-PCP (W-ROI) | 0.92 | 0.519 | 0.889 | 0.717 | 0.068 | 0.583-0.851 |
| L/C-NP (W-ROI) | 0.58 | 0.815 | 0.750 | 0.782 | 0.062 | 0.661-0.903 |
| HDT-PCP | 10.32 | 0.444 | 0.833 | 0.648 | 0.071 | 0.510-0.787 |
| HDT-CMP | 18.52 | 0.889 | 0.667 | 0.814 | 0.054 | 0.707-0.920 |
| HDT-NP | 18.90 | 0.556 | 0.778 | 0.664 | 0.074 | 0.519-0.808 |

S-ROI, small region-of-interest; M-ROI, medium region-of-interest; L-ROI, large region-of-interest; W-ROI, whole region-of-interest; RO, renal oncocytoma; chRCC, chromophobe renal cell carcinoma; AVT, attenuation value of tumor; L/C, the ratio of lesiontocortex attenuation; PCP, pre-contrast phase; CMP, corticomedullary phase; NP, nephrographic phase; HDT, heterogeneous degree of tumor; ROC, receiver operating characteristic; AUC, area under curve; SE, Standard error; CI, confidence interval.

parenchyma possible. These differences in ROI placement approaches used among these studies contributed to significant differences in the comparison of the degree of enhancement for RO and ccRCC lesions. In addition, while studies using different ROIs have all reported a higher enhancement degree for ROs relative to chRCCs, the actual diagnostic performance of the ROI-based enhancement degree-related parameters has been variable.[15-19] Therefore, different ROIs will impact the role of quantitative CT parameters in differential diagnosis, underscoring the need for clear reference criteria for use in clinical practice. For the reasons discussed earlier, the present study employed 4 different ROIs and showed that the most reliable enhancement degree-related parameters for differentiating ROs from ccRCCs and chRCCs were L/C-CMP (S-ROI) and AVT-NP (S-ROI), respectively, which were all obtained by S-ROI. M-ROIs and L-ROIs likely included micronecrotic areas and regions with limited blood supply owing to their larger size, so S-ROIs could maximize the differences between ROs and RCCs.[20]

This analysis revealed that the L/C-CMP (S-ROI) was significantly below the optimal cut-off value (0.99) in most ROs (22/27, 81.48%), whereas it was significantly higher than this cut-off threshold in most ccRCCs (58/74, 78.38%). However, the heterogeneity of the results in different studies using S-ROI to differentiate ROs from ccRCCs demonstrated the poor reproducibility of the results. Gaudiano et al.[21] also used a small ROI (15-20 mm$^2$) and found a higher enhancement change in ccRCCs compared to ROs but without a statistically significant difference. Ren et al.[5] also used a small (8-15 mm$^2$) ROI and reported a more pronounced enhancement change in ccRCCs compared to ROs, with an optimal L/C cut-off of 1.0, which was similar to this study. However, Moldovanu et al.[22] used a small ROI (10 mm$^2$) and observed a higher enhancement change for ROs relative to ccRCCs, but found this difference to not be statistically significant. These studies suggest that the differences in the enhancement degree of ROs and ccRCCs are really very small so that any minimum variability due to technical factors can create a wide overlap of the values. For example, image slice thickness, ROI size, placement position, and enhanced scanning time can all affect the differences in enhancement degree between ROs and ccRCCs. Therefore, it is

**Tables 4.** Logistic regression analysis for differentiation of RO and RCC

| Model | Coefficient | Odds ratio (95% CI) | P | Cox & Snell R² | Nagelkerke R² |
|---|---|---|---|---|---|
| Differentiation of RO and ccRCC | | | | | |
| Constant | −10.464 | | <.001 | 0.374 | 0.545 |
| L/C-CMP (S-ROI) | 4.577 | 97.264 (2.936-3222.043) | .010 | | |
| HDT-PCP | 0.371 | 1.450 (1.150-1.828) | .002 | | |
| Differentiation of RO and chRCC | | | | | |
| Constant | 13.030 | | <.001 | 0.529 | 0.711 |
| AVT-NP (S-ROI) | −0.091 | 0.913 (0.870-0.958) | <.001 | | |
| HDT-CMP | −0.149 | 0.862 (0.757-0.982) | .25 | | |

RO, renal oncocytoma; RCC, renal cell carcinoma; ccRCC, clear cell renal cell carcinoma; chRCC, chromophobe renal cell carcinoma; L/C, the ratio of lesiontocortex attenuation; CMP, corticomedullary phase; S-ROI, small region-of-interest; HDT, heterogeneous degree of tumor; PCP, pre-contrast phase; AVT, attenuation value of tumor; NP, nephrographic phase; CI, confidence interval.

not reliable to differentiate between ROs and ccRCCs only by the CT enhancement features. In contrast, the differentiation between ROs and chRCCs was simpler and in most cases possible in clinical practice based on the evaluation of the enhancement degree of these tumors on contrast-enhanced CT images.[15-19] The present study concluded that AVT-NP (S-ROI) was the most reliable quantitative CT parameter for use when differentiating between ROs and chRCCs, with optimal cut-off and AUC values being 104.5 HU and 0.918, respectively.

SD of CT values has been used as a quantitative parameter to assess the heterogeneity of tumors to differentiate between AML and RCC or among RCC subtypes.[10,23,24] However, in prior studies, tumor heterogeneity when differentiating between ROs and RCCs has largely been based upon the subjective judgment of each radiologist.[4,7-8] The present study showed that HDT-CMP was the most reliable heterogeneity-related parameter for use in differentiating ROs from ccRCCs and chRCCs. Specifically, the HDT-CMP was significantly below the optimal cut-off value (30.19) for most ROs (21/27, 77.78%), whereas it was above this value for most ccRCCs (60/74, 81.08%). HDT-CMP was similarly significantly higher than the optimal cut-off value of 18.52 for most ROs (24/27, 88.89%), whereas it was below this value for most chRCCs (24/36, 66.67%). ccRCCs are known to be the most common type of renal tumors exhibiting heterogeneous enhancement.[25] The hypervascular characteristics in CMP and common necrotic changes can maximize the differences between average values and most individual pixel values in the selected ROI for ccRCC. In contrast, ROs and chRCCs generally exhibited homogeneous enhancement, resulting in smaller HD values. As such, ccRCCs exhibit the highest SD value in CMP. There are 2 possible reasons for the higher HD values in CMP for ROs as compared to chRCCs: the hypervascular characteristics of ROs and the presence of central scar in a small proportion of ROs.[26] In summary, the SD of CT values can be used as a convenient quantitative parameter to differentiate ROs from ccRCCs and chRCCs.

In logistic regression analyses, S-ROI-based enhancement degree parameters and W-ROI-based heterogeneity parameters were identified as the most reliable metrics for differentiating ROs from ccRCCs and chRCCs. Therefore, a combined assessment of both heterogeneity and enhancement degree is integral for reliable differential diagnosis. The predictive models developed to differentiate among these lesion types exhibited excellent efficacy when these 2 quantitative parameters were combined (RO vs. ccRCC: AUC = 0.908 (95% CI: 0.840-0.976); RO vs. chRCC: AUC = 0.944 (95% CI: 0.894-0.995)). The developed models also exhibited similar diagnostic performance in the validation cohort (RO vs. ccRCC: AUC = 0.876; RO vs. chRCC: AUC = 0.959). However, given the extreme variability between these results and prior studies, particularly when differentiating ROs from ccRCCs,[5,21-22] the true clinical value of these models has yet to be established. Even so, these results are of great value to clinical practice for several reasons. First of all, subjective CT morphological features and other quantitative parameters (including central stellate scar, segmental enhancement inversion, necrotic components, calcification within the tumor, and absolute deenhancement) also play an important role in the differentiation of ROs and RCCs, and the present results can serve as important diagnostic criteria in this context.[7,25,26] Second, the combination of multiple imaging techniques can help to more accurately classify renal tumors. For example, magnetic resonance imaging (MRI) is currently rated as being comparable to CT when evaluating renal tumors. Multiparametric MRI, which consists of functional and conventional morphologic imaging, such as dynamic gadolinium chelate-enhanced MRI, dual-echo chemical shift MRI, and diffusion-weighted imaging, can provide a wealth of information for the diagnosis of renal tumors.[25-27] Third, percutaneous renal lesions biopsy is currently accurate and associated with low complication rates.[28] When the models developed herein predict that the lesion may be an RO, renal lesions biopsy may thus be performed, particularly for patients with complications that increase the risk of undergoing surgery.

There are certain limitations to this analysis. First, this was a retrospective study and it is thus susceptible to selection bias. Second, there is potential for error in ROI placement depending on observer assessments, especially when S-ROIs are placed on an image with a 5 mm slice thickness. Theoretically, when using an S-ROI, images with thinner slice thicknesses may help to ensure the accuracy of ROI placement and the reliability of the quantitative data obtained, particularly for small renal tumors. As some cases from this institution only included images with a slick thickness of 5 mm, we had to measure all CT parameters on images with a 5 mm slice thickness to ensure this study would incorporate a sufficient number of cases, particularly for the RO group. In addition, SD values measured on images with different slice thicknesses also differ, highlighting the need for further research. Third, differences in the contrast agent employed and the enhanced scanning time have the potential to impact these quantitative parameters and associated diagnostic utility. Additional research is thus essential to fully establish the impact of these variables on overall diagnostic performance. Fourth, texture analyses were not conducted in the present study, and further analyses of the relationships between HDT and texture analysis results are warranted. Fifth, owing to space limitations, tumor morphological features were not included in this study.

In summary, tumor quantitative parameters that reflect differences in enhancement degree and tumor heterogeneity can be utilized to differentiate ROs from ccRCCs and chRCCs during routine differential diagnosis in the clinic.

## Conflict of interest disclosure

The authors declared no conflicts of interest.

## References

1. Schieda N, Lim RS, McInnes MDF, et al. Characterization of small (<4 cm) solid renal masses by computed tomography and magnetic resonance imaging: current evidence and further development. *Diagn Interv Imaging*. 2018;99(7-8):443-455. [CrossRef]
2. Sasaguri K, Takahashi N, Gomez-Cardona D, et al. Small (<4 cm) renal mass: differentiation of oncocytoma from renal cell carcinoma on biphasic contrast-enhanced CT. *AJR Am J Roentgenol*. 2015;205(5):999-1007. [CrossRef]
3. Meagher MF, Lane BR, Capitanio U, et al. Comparison of renal functional outcomes of active surveillance and partial nephrectomy in the management of oncocytoma. *World J Urol*. 2021;39(4):1195-1201. [CrossRef]
4. Gentili F, Bronico I, Maestroni U, et al. Small renal masses (≤4 cm): differentiation of oncocytoma from renal clear cell carcinoma using ratio of lesion to cortex attenuation and aorta-lesion attenuation difference (ALAD) on contrast-enhanced CT. *Radiol Med*. 2020;125(12):1280-1287. [CrossRef]
5. Ren A, Cai F, Shang YN, et al. Differentiation of renal oncocytoma and renal clear cell carcinoma using relative CT enhancement ratio. *Chin Med J (Engl)*. 2015;128(2):175-179. [CrossRef]
6. Grajo JR, Terry RS, Ruoss J, et al. Using aorta-lesion-attenuation difference on preoperative contrast-enhanced computed tomography scan to differentiate between malignant and benign renal tumors. *Urology*. 2019;125:123-130. [CrossRef]
7. Lee-Felker SA, Felker ER, Tan N, et al. Qualitative and quantitative MDCT features for differentiating clear cell renal cell carcinoma from other solid renal cortical masses. *AJR Am J Roentgenol*. 2014;203(5):W516-W524. [CrossRef]
8. Paño B, Soler A, Goldman DA, et al. Usefulness of multidetector computed tomography to differentiate between renal cell carcinoma and oncocytoma. A model validation. *Br J Radiol*. 2020;93(1115):20200064. [CrossRef]
9. Rosenkrantz AB, Matza BW, Portnoy E, Melamed J, Taneja SS, Wehrli NE. Impact of size of region-of-interest on differentiation of renal cell carcinoma and renal cysts on multi-phase CT: preliminary findings. *Eur J Radiol*. 2014;83(2):239-244. [CrossRef]
10. Wang X, Song G, Jiang H. Differentiation of renal angiomyolipoma without visible fat from small clear cell renal cell carcinoma by using specific region of interest on contrast-enhanced CT: a new combination of quantitative tools. *Cancer Imaging*. 2021;21(1):47. [CrossRef]
11. Allgood E, Raman SS. Image interpretation: practical triage of benign from malignant renal masses. *Radiol Clin North Am*. 2020;58(5):875-884. [CrossRef]
12. Nicolau C, Antunes N, Paño B, Sebastia C. Imaging characterization of renal masses. *Medicina (Kaunas)*. 2021;57(1). [CrossRef]
13. Young JR, Margolis D, Sauk S, Pantuck AJ, Sayre J, Raman SS. Clear cell renal cell carcinoma: discrimination from other renal cell carcinoma subtypes and oncocytoma at multiphasic multidetector CT. *Radiology*. 2013;267(2):444-453. [CrossRef]
14. Bird VG, Kanagarajah P, Morillo G, et al. Differentiation of oncocytoma and renal cell carcinoma in small renal masses (<4 cm): the role of 4-phase computerized tomography. *World J Urol*. 2011;29(6):787-792. [CrossRef]
15. Grajo JR, Batra NV, Bozorgmehri S, et al. Validation of aorta-lesion-attenuation difference on preoperative contrast-enhanced computed tomography scan to differentiate between malignant and benign oncocytic renal tumors. *Abdom Radiol (NY)*. 2021;46(7):3269-3279. [CrossRef]
16. Guo K, Ren S, Cao Y, et al. Differentiation between renal oncocytomas and chromophobe renal cell carcinomas using dynamic contrast-enhanced computed tomography. *Abdom Radiol (NY)*. 2021;46(7):3309-3316. [CrossRef]
17. Li X, Nie P, Zhang J, Hou F, Ma Q, Cui J. Differential diagnosis of renal oncocytoma and chromophobe renal cell carcinoma using CT features: a central scar-matched retrospective study. *Acta Radiol*. 2022;63(2):253w-260. [CrossRef]
18. Wu J, Zhu Q, Zhu W, Chen W, Wang S. Comparative study of CT appearances in renal oncocytoma and chromophobe renal cell carcinoma. *Acta Radiol*. 2016;57(4):500-506. [CrossRef]
19. Choi JH, Kim JW, Lee JY, et al. Comparison of computed tomography findings between renal oncocytomas and chromophobe renal cell carcinomas. *Korean J Urol*. 2015;56(10):695-702. [CrossRef]
20. Zhang J, Lefkowitz RA, Ishill NM, et al. Solid renal cortical tumors: differentiation with CT. *Radiology*. 2007;244(2):494-504. [CrossRef]
21. Gaudiano C, Schiavina R, Vagnoni V, et al. Can the multiphasic computed tomography be useful in the clinical management of small renal masses? *Acta Radiol*. 2017;58(5):625-633. [CrossRef]
22. Moldovanu CG, Petresc B, Lebovici A, et al. Differentiation of clear cell renal cell carcinoma from other renal cell carcinoma subtypes and benign oncocytoma using quantitative MDCT enhancement parameters. *Medicina (Kaunas)*. 2020;56(11). [CrossRef]
23. Jung SC, Cho JY, Kim SH. Subtype differentiation of small renal cell carcinomas on three-phase MDCT: usefulness of the measurement of degree and heterogeneity of enhancement. *Acta Radiol*. 2012;53(1):112-118. [CrossRef]
24. Leng S, Takahashi N, Gomez Cardona D, et al. Subjective and objective heterogeneity scores for differentiating small renal masses using contrast-enhanced CT. *Abdom Radiol (NY)*. 2017;42(5):1485-1492. [CrossRef]
25. Sasaguri K, Takahashi N. CT and MR imaging for solid renal mass characterization. *Eur J Radiol*. 2018;99:40-54. [CrossRef]
26. Cornelis F, Lasserre AS, Tourdias T, et al. Combined late gadolinium-enhanced and double-echo chemical-shift MRI help to differentiate renal oncocytomas with high central T2 signal intensity from renal cell carcinomas. *AJR Am J Roentgenol*. 2013;200(4):830-838. [CrossRef]
27. Akın IB, Altay C, Güler E, et al. Discrimination of oncocytoma and chromophobe renal cell carcinoma using MRI. *Diagn Interv Radiol*. 2019;25(1):5-13. [CrossRef]
28. Dhyani M, Grajo JR, Rodriguez D, et al. Aorta-lesion-attenuation-difference (ALAD) on contrast-enhanced CT: a potential imaging biomarker for differentiating malignant from benign oncocytic neoplasms. *Abdom Radiol (NY)*. 2017;42(6):1734-1743. [CrossRef]